Conformational stability of ribonuclease T1 determined by hydrogen–deuterium exchange

LEISHA S. MULLINS,[1] C.N. PACE,[2] AND FRANK M. RAUSHEL[1]

[1]Department of Chemistry, Texas A & M University, College Station, Texas 77843
[2]Medical Biochemistry and Genetics, Texas A & M University, College Station, Texas 77843

Abstract

The hydrogen–deuterium exchange kinetics of 37 backbone amide residues in RNase T1 have been monitored at 25, 40, 45, and 50 °C at pD 5.6 and at 40 and 45 °C at pD 6.6. The hydrogen exchange rate constants of the hydrogen-bonded residues varied over eight orders of magnitude at 25 °C with 13 residues showing exchange rates consistent with exchange occurring as a result of global unfolding. These residues are located in strands 2–4 of the central β-pleated sheet. The residues located in the α-helix and the remaining strands of the β-sheet exhibited exchange behaviors consistent with exchange occurring due to local structural fluctuations. For several residues at 25 °C, the global free energy change calculated from the hydrogen exchange data was over 2 kcal/mol greater than the free energy of unfolding determined from urea denaturation experiments. The number of residues showing this unexpected behavior was found to increase with temperature. This apparent inconsistency can be explained quantitatively if the *cis-trans* isomerization of the two *cis* prolines, Pro-39 and Pro-55, is taken into account. The *cis-trans* isomerization equilibrium calculated from kinetic data indicates the free energy of the unfolded state will be 2.6 kcal/mol higher at 25 °C when the two prolines are *cis* rather than *trans* (Mayr LM, Odefey CO, Schutkowski M, Schmid FX. 1996. Kinetic analysis of the unfolding and refolding of ribonuclease T1 by a stopped-flow double-mixing technique. *Biochemistry 35*: 5550–5561). The hydrogen exchange results are consistent with the most slowly exchanging hydrogens exchanging from a globally higher free energy unfolded state in which Pro-55 and Pro-39 are still predominantly in the *cis* conformation. When the conformational stabilities determined by hydrogen exchange are corrected for the proline isomerization equilibrium, the results are in excellent agreement with those from an analysis of urea denaturation curves.

Keywords: hydrogen–deuterium exchange; NMR; protein folding; ribonuclease T1

The principal factors governing the conformational stability of proteins in solution are still not fully understood. While traditional methods of denaturant titration and calorimetry provide valuable information on global stability, no direct information on the conformational dynamics in solution is gained. The internal mobility of proteins can be measured, however, by following the hydrogen–deuterium exchange (HX) kinetics of individual backbone amide hydrogens. Hydrogen exchange experiments take advantage of the fact that buried or hydrogen-bonded protons exchange with solvent several orders of magnitude more slowly than exposed or non-hydrogen-bonded protons. More importantly, large differences are also observed in the exchange kinetics of hydrogen-bonded residues. These differences are a direct reflection of the local stability in the region of the hydrogen bond, thus allowing an assessment of the rigidity or the flexibility in the area around the hydrogen bond. Therefore, measuring the hydrogen exchange kinetics of individual residues in a protein provides detailed structural stability information at the residue level.

A general two-step model has been proposed to account for hydrogen exchange with solvent in a folded protein (Linderstrøm-Lang, 1955; Hvidt & Nielsen, 1966; Woodward et al., 1982; Englander & Kallenbach, 1984; Englander & Mayne, 1992; Bai et al., 1994; Loh et al., 1996). In this model, there is an equilibrium between two sets of protein conformations, *closed* and *open*, where solvent exchange only takes place from the open form (Bai et al., 1994).

$$\text{Closed} \underset{k_{cl}}{\overset{k_{op}}{\rightleftharpoons}} \text{Open} \xrightarrow{k_{int}} \text{Exchange}. \tag{1}$$
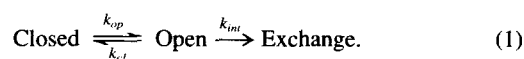
Under conditions that favor the closed conformations, $k_{cl} \gg k_{op}$, the observed rate constant for exchange, k_{ex}, is $k_{int}(k_{op}/k_{cl})$ if conformational closing is faster than solvent exchange from the open state, $k_{cl} \gg k_{int}$. The intrinsic rate of exchange from the open state, k_{int}, can be predicted from unstructured peptide data, thus allowing

the determination of the equilibrium constant and the standard free energy change for the opening reaction (Molday et al., 1972; Connelly et al., 1993; Bai et al., 1993):

$$k_{ex} = k_{int}(k_{op}/k_{cl}) = k_{int}K_{op} \quad \text{when } k_{cl} \gg k_{int}, \qquad (2)$$

$$K_{op} = k_{ex}/k_{int} \qquad (3)$$

and

$$\Delta G_{op}^{\circ} = -RT \ln(k_{ex}/k_{int}). \qquad (4)$$

In this model, the two limiting cases for exchange are limited local fluctuations and complete global unfolding (Kim & Woodward, 1993). The slowest exchanging amides are generally assumed to exchange by the global unfolding pathway, and the faster exchanging amides through local fluctuations (Kim et al., 1993; Mayo & Baldwin, 1993; Bai et al., 1994). If hydrogen exchange occurs only by globally unfolding, then the free energy of opening, ΔG_{op}°, calculated from HX experiments, should be similar to the free energy change determined from denaturation experiments, ΔG_{u}°, when the respective unfolded states are similar (Loh et al., 1993; Swint-Kruse & Robertson, 1996). For the slowest exchanging amides in a number of proteins, this is indeed the case (Loh et al., 1993; Jeng & Dyson, 1995, Orban et al., 1995; Perrett et al., 1995; Swint-Kruse & Robertson, 1996). When exchange occurs from local structural fluctuations, the resultant ΔG_{op}° can be smaller than ΔG_{u}° because exchange would occur from an intermediate not necessarily dependent on global stability (Kim & Woodward, 1993). The two exchange limits are also distinguishable by their temperature dependence (Kim & Woodward, 1993; Orban et al., 1995; Swint-Kruse & Robertson, 1996). To investigate these two limits, the hydrogen exchange kinetics of ribonuclease T1 (RNase T1) have been determined under a variety of conditions.

RNase T1 is an extremely well characterized small globular protein of 104 amino acids with a single hydrophobic core formed between a 4.5-turn α-helix and an antiparallel β-sheet (Martinez-Oyanedel et al., 1991). RNase T1 has four prolines, two of which are in the *cis* conformation in the native structure (Pace et al., 1991). The energetics and the kinetics of folding of wild type RNase T1 have been extensively characterized with the refolding kinetics showing two slow refolding phases caused by proline isomerization (Pace et al., 1991; Hu et al., 1992; Kiefhaber et al., 1990a, 1990b, 1990c, 1992a, 1992b; Mayr et al., 1996). Even though the refolding kinetics are very slow (7,000 s for the slowest phase at pH 5, 10 °C) and are dominated by proline isomerization, it has been shown by rapid quench–hydrogen exchange that there is a very rapid formation of secondary structure within 100 ms of refolding (Mullins et al., 1993). Woodward (1993) has suggested that a relationship exists between the slowest exchanging amide protons and the folding core of a protein. This interrelationship between the rapid formation of secondary structure and the hydrogen exchange kinetics has now been examined in some detail with RNase T1.

Results

The HX exchange rates of 37 backbone amide residues in RNase T1 were measured at 25, 40, 45, and 50 °C in 25 mM acetate-d_3 D_2O buffer, pD = 5.6 (pD = pH$_{meter}$ + 0.4). The exchange reactions were followed by 2D-COSY NMR spectroscopy for time

periods ranging from 14 h (50 °C) to over 1 yr (25 °C). The backbone amide proton assignments of Hoffmann and Rüterjans (1988) were used and any shifts due to temperature or pH were verified by standard sequential assignment techniques. The rate constants for the HX exchange (k_{ex}), shown in Table 1, range from 9×10^{-2} to 1×10^{-9} h^{-1} at 25 °C. Residues not listed either exchanged within the deadtime of the experiment (20 min) or were involved in ambiguous resonance assignments due to overlapping peaks. The error in the measured rate constants did not exceed 10% of the reported value as determined by a fit to a single exponential function, $A = A_0[\exp(-kt)] + C$. Of the 37 residues followed, the fastest and slowest to exchange are S12 and I61, respectively. For 13 residues, Y11, Y57, W59, I61, D77, V78, V79, F80, N81, Q85, A87, T91, and V101, the rates of exchange were too slow to be measured with the experimental conditions used at 25 °C, so the HX rates were calculated by extrapolation from the higher temperature HX data using an activation energy of 103 kcal/mol, which was determined from standard Arrhenius plots (refer to Fig. 1).

The intensities of the COSY NH-CαH crosspeaks for the slowest exchanging amides at 25 °C, pD 5.6 were significantly depressed (up to 50%) relative to 90% H_2O control samples when the exchange reaction was started from direct incubation of the lyophilized protein into the exchange buffer (data not shown). The decreased crosspeak intensity is most likely due to a structural isomerization that occurs as a result of the dehydration process, which is reversible under solvating conditions. Complications due to this process were avoided by incubation of the lyophilized protein in water for at least 24 h prior to diafiltration into the exchange buffer, at which point the observed COSY crosspeak intensities at the initial time points for the slowest exchanging amides were comparable to the 90% H_2O control samples.

The intrinsic rates of exchange from the denatured state (k_{int}) were calculated using the method of Bai et al. (1993), utilizing an
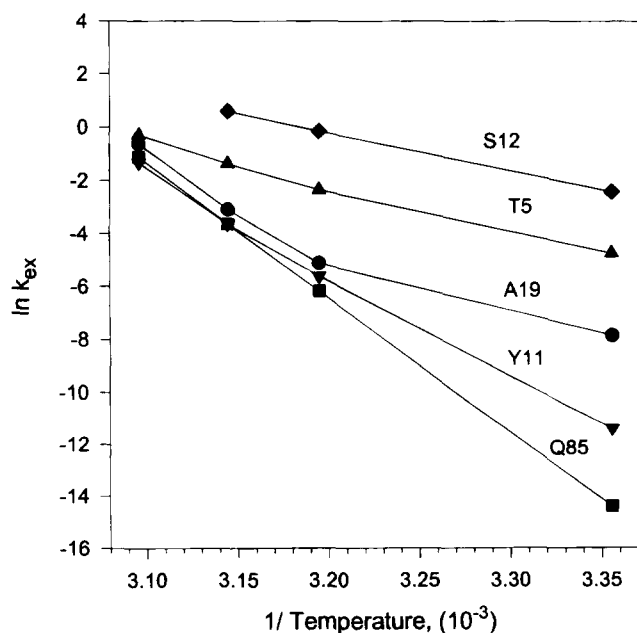

Fig. 1. Temperature dependence of hydrogen exchange rate constants at pD = 5.6: (♦) S12, (▲) T5, (●) A19, (▼) Y11, (■) Q85.

**Table 1.** *Ribonuclease T1 amide exchange: k_{ex} data in hours^{-1}*

	pD = 5.6				pD = 6.6	
	25 °C	40 °C	45 °C	50 °C	40 °C	45 °C
Y 4	4.47E−04	7.37E−03	2.40E−02	2.20E−01	6.19E−02	5.46E−01
T 5	8.50E−03	9.41E−02	2.50E−01	7.40E−01	6.00E−01	1.92
C 6[a]	5.50E−03	9.12E−02	1.90E−01	3.90E−01	8.0E−01	4.44E−01
Y 11	1.11E−05[b]	3.61E−03	2.60E−02	2.60E−01	7.05E−02	7.79E−01
S 12	8.70E−02	8.54E−01	1.8	DT[c]	DT	DT
V 16	7.30E−04	1.35E−02	2.40E−02	1.60E−01	6.28E−02	4.00E−01
S 17	6.67E−04	5.91E−02	1.54E−01	DT	4.39E−01	DT
A 19	3.80E−04	5.91E−03	4.50E−02	5.30E−01	1.50E−01	8.86E−01
Q 20	2.70E−04	2.35E−03	2.80E−02	DT	DT	DT
A 21	3.02E−04	7.85E−03	2.60E−02	DT	DT	DT
A 22	2.80E−04	4.81E−03	2.80E−02	3.40E−01	1.00E−01	1.08
Y 24	3.98E−04	1.61E−03	3.30E−02	DT	DT	DT
K 25	2.40E−03	7.82E−02	1.60E−01	DT	DT	DT
L 26	1.70E−04	1.41E−02	4.00E−02	2.40E−01	2.52E−01	1.66
H 40	1.10E−03	6.36E−02	1.50E−01	9.70E−01	4.77E−01	2.59
Y 42	2.07E−02	DT	DT	DT	DT	DT
Y 57	2.42E−06[b]	1.35E−03	9.80E−03	1.60E−01	4.39E−02	3.50E−01
E 58	6.58E−04	2.46E−03	9.80E−03	2.74E−01	4.61E−02	4.96E−01
W 59	4.29E−07[b]	1.10E−03	1.40E−02	1.40E−01	2.72E−02	3.08E−01
I 61	9.51E−08[b]	4.93E−04	4.80E−03	8.70E−02	2.05E−02	3.09E−02
L 62	5.50E−04	1.36E−02	4.00E−02	2.70E−01	1.59E−01	6.89E−01
D 76	1.40E−02[b]	2.67E−01	5.70E−01	1.4	DT	DT
R 77	2.82E−07[b]	1.17E−03	1.90E−02	2.00E−01	5.16E−02	3.85E−01
V 78	3.24E−07[b]	6.10E−04	1.00E−02	2.40E−01	4.27E−02	4.2E−01
V 79	1.37E−07[b]	1.90E−03	6.70E−03	1.20E−01	2.64E−02	3.56E−01
F 80	3.35E−07[b]	1.33E−03	1.30E−02	2.30E−01	5.29E−02	5.30E−01
N 81	1.90E−06[b]	3.63E−03	3.20E−02	3.60E−01	9.20E−02	1.00
N 84	1.40E−03	2.17E−02	6.50E−02	4.60E−01	2.10E−01	1.81
Q 85	5.53E−07[b]	2.05E−03	2.60E−02	3.20E−01	7.91E−02	7.28E−01
A 87	9.35E−07[b]	2.21E−03	1.30E−02	2.30E−01	5.59E−02	4.82E−1
G 88	ND[d]	2.05E−03	2.90E−02	DT	1.04E−01	DT
V89	2.01E−02	ND	2.0E−01	DT	1.21E−01	DT
I 90	1.16E−04	1.77E−03	8.80E−03	1.53E−01	3.64E−02	3.84E−01
T 91	3.99E−06[b]	4.75E−03	2.70E−02	3.40E−01	8.48E−02	9.73E−01
H 92	1.17E−03	5.46E−02	1.50E−01	1.4	2.69E−01	DT
V 101	4.13E−06[b]	2.65E−03	1.60E−02	1.40E−01	4.73E−02	4.44E−01
C 103	5.10E−03	4.20E−02	1.20E−01	5.10E−01	2.58E−01	1.14

[a]The crosspeaks for C6 and F100 overlap and by default are labeled C6.
[b]Rate constants calculated by extrapolation from higher temperatures.
[c]Exchange complete in experimental deadtime—20 min.
[d]Rate constants not determined.

Excel spreadsheet kindly provided by Dr. Andrew Robertson (University of Iowa). The protection factor, k_{int}/k_{ex}, for each residue was calculated and a plot of the protection factor relative to the residue number is shown in Figure 2. The single α-helix is located between residues 13 and 30 and the five-stranded central β-sheet from residues 39–43, 55–63, 76–82, 85–92 and 100–103. The 37 residues that were followed show protection factors of 10^4 to 10^9 based on the calculated intrinsic exchange rates. It is of interest to note that although I61 is the slowest amide to exchange, Q85 shows the greatest degree of protection from exchange. As expected from the HX rate constants, k_{ex}, the residues comprising the central β pleated sheet show 10^3 greater protection from exchange than the residues in the helix, and the overall degree of protection decreases with increasing temperature (Table 1).

The free energy of opening, ΔG_{op}°, can be calculated from the rate constants for amide exchange, k_{ex}, and the intrinsic rates of exchange, k_{int}, using Equation 4. At 25 °C, the calculated ΔG_{op}° values reveal a range of stability from 5.5 to 12.5 kcal/mol at individual residues (Table 2). The free energy of opening for ten of the residues is greater by 1–2 kcal/mol than the global free energy previously determined from either urea denaturation or thermodynamic data (Hu et al., 1992; Yu et al., 1994). The number of residues showing this unexpected behavior increases with temperature, and at 50 °C all 37 residues have values for ΔG_{op}° that are greater than the global free energy determined from thermodynamic data (Hu et al., 1992; Yu et al., 1994). To calculate ΔG_{op}° as shown in Equation 4, the rate of conformational closing must be greater than exchange from the open state, $k_{cl} \gg k_{int}$. This is the so-called EX2 limit. If, however, the rate of conformational closing is less than the intrinsic rate of exchange, $k_{cl} \ll k_{int}$, then at this EX1 limit, the observed rate of exchange, k_{ex}, would be the rate of the opening reaction, k_{op} (i.e., $k_{ex} = k_{op}$) (Hvidt & Nielsen, 1966).
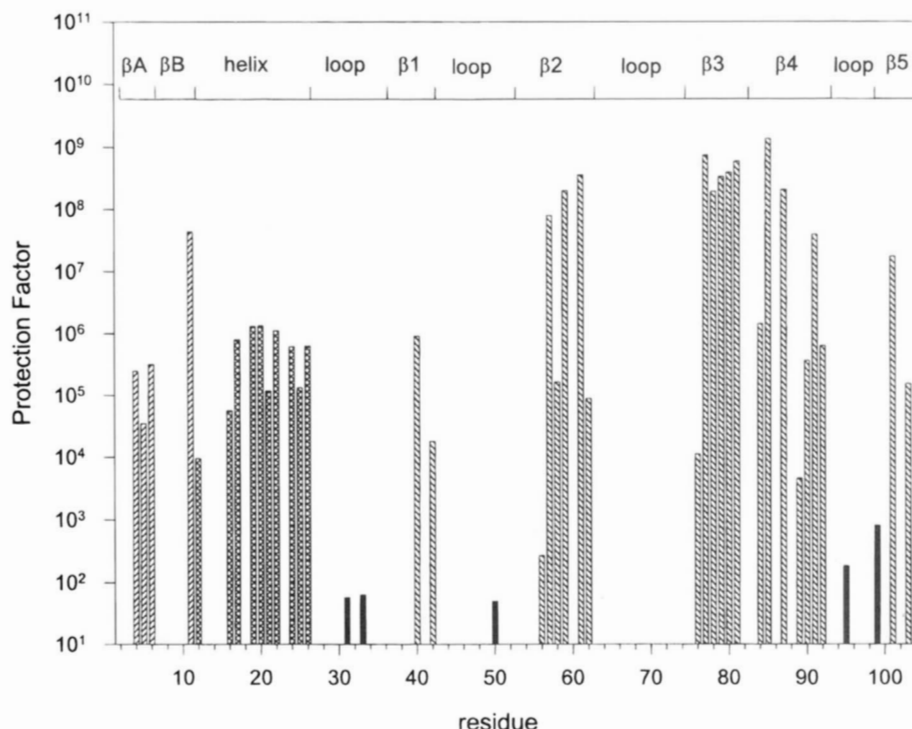
Fig. 2. Protection factors determined at 25 °C for the backbone amide hydrogens of RNase T1 as a function of residue number. Black bars indicate residues where exchange was essentially complete in the deadtime of the experiment.

It is thus impossible to obtain information on the equilibrium constant for the opening reaction and the free energy of opening when exchange occurs from the EX1 limit. Exchange behavior between the EX1 and EX2 limits can be described by the following equation (Hvidt & Nielsen, 1966):

$$k_{ex} = \frac{k_{op}k_{int}}{k_{cl} + k_{int}}. \qquad (5)$$

Under these intermediate conditions, the apparent free energy of the opening reaction can be higher than ΔG_u°. The EX1 and EX2 limits are distinguishable by their pH dependence (Bai et al., 1994; Clark & Fersht, 1996). In the EX1 limit, the rate of exchange is solely dependent on the rate of opening, which is commonly assumed to be independent of pH (Bai et al., 1994). In an effort to determine if the unexpected hydrogen exchange results, which indicated ΔG_{op}° was greater than ΔG_u°, were caused by exchange occurring by an EX1 rather than an EX2 mechanism, the HX experiments were repeated at 40 and 45 °C, pD = 6.4. As seen in Table 1, all the residues show five- to 20-fold increases in the rate of amide exchange as the pH increases one unit, indicating that the exchange mechanism is still EX2. Also, a plot of the logarithm of the exchange rates at pD 5.6 against pD 6.6 shows a slope near unity which also indicates there is no deviation from an EX2 mechanism.

Proteins generally exhibit increased stability in D_2O (Swint & Robertson, 1993). For this reason, urea denaturation studies were performed to determine the stability of RNase T1 in D_2O under the conditions identical to those used for the HX experiments. The free energy of stabilization, ΔG_u° (D_2O) of RNase T1 at pD = 5.6 is 6.9, 5.5, and 4.4 kcal/mol and 40, 45, and 50 °C, respectively.

Discussion

Relationship between hydrogen exchange and structure

To gain insight into hydrogen exchange and the conformational equilibria of the folded state that govern exchange, the information obtained from the HX experiments should be discussed in terms of the three-dimensional structure of the protein. Figures 3 and 4 show the location of the amide residues followed in this experiment mapped on the secondary and tertiary structure of RNase T1. All amide hydrogens not involved in backbone–backbone or backbone–side-chain hydrogen bonds exchanged within the deadtime of the experiment, with the exception of L62, D76, and V89. Structurally, residues L62 and D76 are terminating residues in β-strands and V89 is in the middle of a β-strand. As observed in the crystal structure solved by Martinez-Oyanedel et al. (1991), all three residues form hydrogen bonds with water molecules, two of which have been identified as conserved waters (Malin et al., 1991). Several residues, T5, V16, and Y42, which make backbone–backbone hydrogen bonds, and one, S12, which makes a backbone–side-chain hydrogen bond, also have protection factors in the range determined for L62, D76, and V89. These residues are also found either near the terminus of a secondary structural element or in small spans of localized structure. The protection factors in the range of 10^4 seen for L62, D76, and V89 are a possible result of the hydrogen-bonding network in the secondary structures in which the residues participate or could be due to a hydrogen bond with a structural water. This range of protection has been observed for N-terminal α-helical residues in other proteins such as staphylococcal nuclease and hen egg-white lysozyme (Loh et al., 1993; Radford et al., 1992).

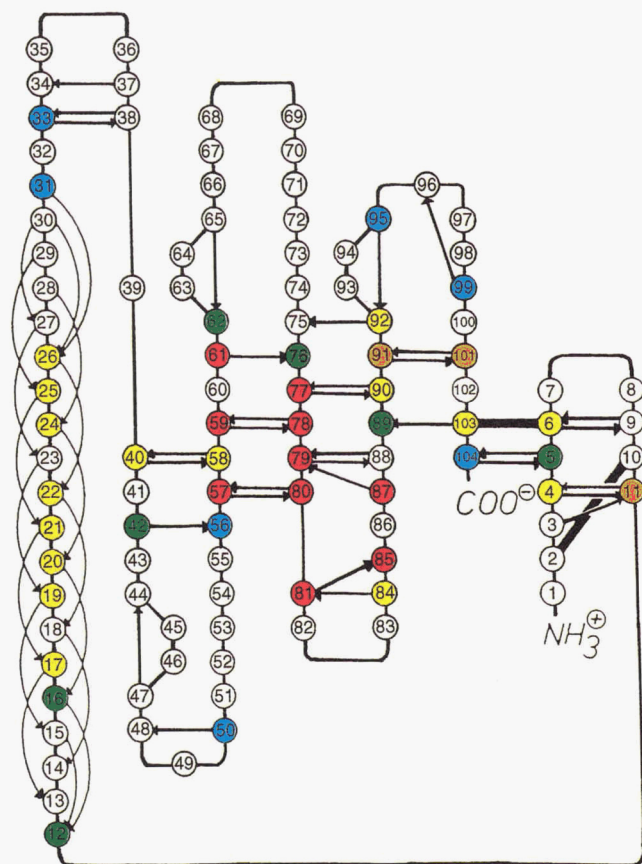**Table 2.** *Unfolding free energies from HX experiments*

	pD = 5.6				pD = 6.6	
	25 °C	40 °C	45 °C	50 °C	40 °C	45 °C
Y 4	7.36	6.84	6.71	5.69	7.04	6.05
T 5	6.20	5.87	5.85	5.55	6.25	5.88
C 6	7.51	7.00	7.15	7.09	7.17	7.93
Y 11[a]	10.42	8.20	7.59	6.53	7.88	6.76
S 12	5.42	5.13	5.25			
V 16	6.48	5.85	6.08	5.26	6.42	5.62
S17	8.05	6.52	6.52			
A 19	8.34	7.91	7.26	6.08	7.42	6.69
Q 20	8.35	8.28	7.35			
A 21	8.48	7.73	7.60			
A 22	8.25	7.75	7.27	6.07	7.39	6.28
Y 24	7.90	8.29	7.02			
K 25	6.99	6.03	6.18			
L 26	7.92	6.42	6.37	5.62	6.16	5.34
H 40	8.12	6.86	6.93	6.14	7.13	6.45
Y 42	5.49					
Y 57[a]	10.76	8.23	7.61	6.23	7.59	6.67
E 58	7.11	7.51	7.26		7.21	6.10
W 59[a]	11.32	7.87	6.89	5.82	7.40	6.25
I 61[a]	11.66	7.78	6.97	5.52	6.99	7.11
L 62	6.74	5.95	5.86	5.02	5.94	5.38
D 76	5.52	4.82	4.92	4.72		
R 77[a]	12.09	8.38	7.25	6.15	7.54	6.67
V 78[a]	11.30	8.03	6.90	5.26	6.92	5.85
V 79[a]	11.62	7.13	6.95	5.50	7.02	5.76
F 80[a]	11.71	8.01	7.20	5.76	7.24	6.17
N 81[a]	11.95	8.71	7.98	6.85	8.23	7.13
N 84	8.40	7.97	7.91	7.08	8.09	7.13
Q 85[a]	12.45	8.83	7.86	6.67	8.08	7.08
A 87[a]	11.34	7.93	7.44	6.01	7.45	6.48
G 88		8.67	7.64		7.75	
V89	4.99					
I 90	7.58	7.13	6.73		6.77	5.66
T 91[a]	10.36	7.33	6.85	5.63	7.06	5.91
H 92	7.92	6.38	6.35	5.31	6.92	
V 101[a]	9.87	7.21	6.69	5.70	6.94	5.91
C 103	7.07	6.98	6.93	6.40	7.37	6.82
HX ΔG°_{op}	11.3	8.0	7.2	6.0	7.4	6.4
Urea ΔG°_{u} H_2O[b]	10.5	6.5	5.1	3.5		
Urea ΔG°_{u} D_2O		6.9	5.5	4.4		

[a]Data used to calculate average ΔG.
[b]C.N. Pace, personal communication.

As seen in Figure 3, there are approximately 50 backbone–backbone amide hydrogen bonds as determined from the crystal structure of RNase T1 solved by Martinez-Oyanedel et al. (1991), with 18 occurring in the α-helix, 23 occurring in the β-sheets, and the remainder in turns. The majority of the turn residues involved in backbone hydrogen bonds as well as the C-terminal residues of the α-helix showed exchange that was almost complete within the deadtime of the experiments (see Fig. 2). The central residues in the α-helix, the residues in strand A (βA) of the small two-stranded β-sheet, and strand 1 (β1) of the central five-stranded β-sheet showed only an order of magnitude greater protection (10^5 to 10^6) than the protection of the residues located near the termini of the secondary structural elements. These results indicate that there is considerable fraying and flexibility in the α-helix and the initial strands of both β-sheets.

All of the 13 "slowest" exchangers at 25 °C are located in strands 2–5 of the central five-stranded β-pleated sheet except Y11, which is in the B strand (βB) of the small sheet. Five of the 13 slowest exchangers (D77, V78, V79, F80, and N81) are in strand 3 (β3), three (Y57, W59, and I61) are in strand 2 (β2), three (Q85, A87, and T91) are in strand 4 (β4), and one (V101) is in strand 5 (β5). The extremely high protection factors of these residues indicate that the central portion of the central β-sheet is extremely rigid. The residues in strand 4 have protection factors ranging from 10^5 to 10^9, making this strand unusual with regard to the range of protection factors observed. The reason for this range is readily apparent upon inspection of the hydrogen-bonding pattern in the three-dimensional structure (Martinez-Oyanedel et al., 1991). The central five-stranded β-pleated sheet is twisted to form a barrel-like structure. The twist is greatest in strand 4 causing a slightly

Fig. 3. Main-chain hydrogen bonding of RNase T1 showing the positions of the slowly exchanging amides colored according to the free energy of opening, ΔG_{op}°: (red) 11–12 kcal/mol ($\Delta G_{op}^{\circ} > \Delta G_u^{\circ}$); (orange) 8–10 kcal/mol ($\Delta G_{op}^{\circ} = \Delta G_u^{\circ}$); (yellow) 6–8 kcal/mol ($\Delta G_{op}^{\circ} < \Delta G_u^{\circ}$); (green) 4–5 kcal/mol ($\Delta G_{op}^{\circ} < \Delta G_u^{\circ}$); (blue) exchange almost complete within deadtime of experiment. Figure adapted from Pace et al. (1991).

The high protection factors in strands 3 and 4 indicate that this region is important to stability. Circular variants of RNase T1 have been made by Garrett et al. (1996) in which new termini were introduced in loop regions while the original N- and C-termini were connected by a short peptide linker. The only loop or turn where new termini could not be introduced was the tight β-turn between strands 3 and 4. This turn is relatively buried with little solvent exposure so it is possible that the introduction of new termini in this area disrupted the hydrogen-bond network in strands 3 and 4 to the extent that the resultant protein was highly unstable. Alternatively, this area may serve as a nucleation site for the initiation of protein folding. High protection factors have also been observed in strands surrounding a buried β-turn in turkey ovomucoid third domain (Swint-Kruse & Robertson, 1996).

Relationship between hydrogen exchange and stability

The standard free energy of the opening reaction, ΔG_{op}°, can be determined from the ratio of the observed rate of hydrogen exchange relative to the calculated intrinsic rate of exchange (k_{ex}/k_{int}) as shown in Equation 4. The best test of whether the most highly protected residues of RNase T1 exchange by global unfolding is a comparison of ΔG_{op}° and ΔG_u°. As seen in Table 2, three residues, Y11, T91, and V101 have an average ΔG_{op}° of 10.2 kcal/mol, which is very close to the ΔG_u° of 10.45 kcal/mol determined by solvent denaturation and calorimetric methods. However, 11 residues showed ΔG_{op}° greater than ΔG_u° at 25 °C. The number of residues showing this unexpected result increases with temperature such that all residues show ΔG_{op}° values greater than ΔG_u° at 50 °C.

Enhanced stability has been observed in a number of proteins and has been explained in a variety of ways. There are three primary explanations for enhanced protection: Residual structure in the denatured state resulting in an over estimation of the intrinsic exchange rate, deviation from EX2 kinetics, or exchange from an intermediate or unfolded state with a higher free energy. Five

irregular hydrogen-bonding pattern around residues G88 and V89 that may cause the lower protection factors of these residues. The greater protection of the β-sheet residues relative to the α-helix residues resembles the distribution of the temperature factors determined from the crystal structure, again indicating that the helix is more flexible than the central β-sheet (Martinez-Oyanedel et al., 1991).
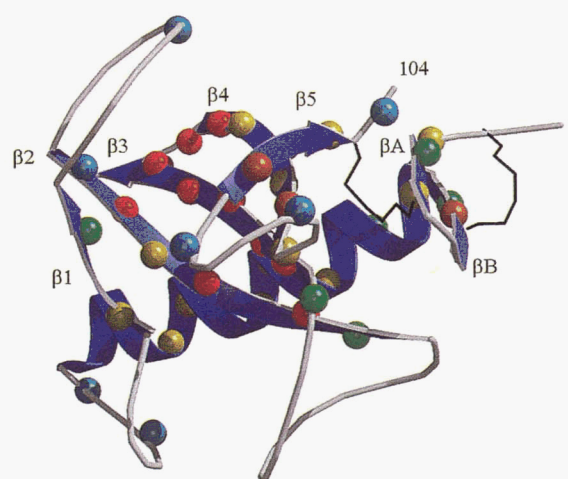
The residue with the highest protection factor is Q85. This is of interest because, in the crystal structure, the amide hydrogen of Q85 makes a tertiary contact with the side chain of N81. If, indeed, this is the most highly protected residue, either it is making a backbone contact not seen in the crystal structure or the side chains of the β-sheet residues are also highly structured. Evidence for limited side chain mobility was observed by Johnson and Raushel (1996) in fluorescence studies on wild-type and circularly permuted RNase T1, which characterized the lifetime, accessibility to quenching, and rotational properties of W59. They found W59 to be extremely buried and the side chain exhibiting a high degree of immobility such that only a single mode of rotation corresponding to diffusion of the entire protein could be detected. The fluorescence lifetimes of W59 are consistent with the high protection factor of Q85 indicating that not only the backbone atoms but also the side-chain atoms are highly ordered with limited mobility.

Fig. 4. Ribbon diagram of native RNase T1 showing the positions of the slowly exchanging amides colored according to the free energy of opening, ΔG_{op}°: (red) 11–12 kcal/mol ($\Delta G_{op}^{\circ} > \Delta G_u^{\circ}$); (orange) 8–10 kcal/mol ($\Delta G_{op}^{\circ} = \Delta G_u^{\circ}$); (yellow) 6–8 kcal/mol ($\Delta G_{op}^{\circ} < \Delta G_u^{\circ}$); (green) 4–5 kcal/mol ($\Delta G_{op}^{\circ} < \Delta G_u^{\circ}$); (blue) exchange almost complete within deadtime of experiment. Figure drawn using MOLSCRIPT (Kraulis, 1991), Raster3D (Merritt & Murphy, 1994) and the coordinates of Martinez-Oyanedel et al. (1991).

residues in the $\beta3$–$\beta4$ hairpin of the B1 domain of protein G exhibit enhanced stability that decreases with increasing temperature, indicating that these residues are involved in residual structure in the "unfolded" state (Orban et al., 1995). As seen in Table 2, the enhanced protection observed for RNase T1 encompasses more residues as the temperature increases. This observation, along with the improbability of an "unfolded" state at 50 °C having more residual structure than the one at 25 °C, argues against residual structure as the primary cause of the enhanced stability seen here for RNase T1. Deviation from EX2 kinetics has been observed for a few residues in turkey ovomucoid third domain, hen egg white lysozyme, and barnase (Radford et al., 1992; Perrett et al., 1995; Swint-Kruse & Robertson, 1996). As discussed in Clark and Fersht (1996), a sensitive method for detecting deviations from EX2 kinetics is an analysis of the relative effect of pD on the exchange rates of all amide protons. A plot of the logarithm of the exchange rates at one pH against those for another pH (alkaline) can distinguish between an EX2 and EX1 mechanism since k_{ex} is proportional to the hydroxide ion concentration (above pH 5) in EX2 kinetics but not in EX1 kinetics. There are no apparent anomalous pH dependencies on the HX kinetics of RNase T1 as seen Table 1, and a plot of k_{ex} at pD 5.6 against pD 6.6 (not shown) shows the same pH dependence for all residues at 40 and 45 °C, with the only possible exceptions being I61 and T5 at 45 °C. Even if minor deviations from EX2 behavior occurred, the apparent ΔG°_{op} would not appreciably differ from the true ΔG°_u. For example, when the rate of closing and the intrinsic rate of exchange are equal, ΔG°_{op} will only be increased 0.4 kcal/mol (Bai et al., 1994). The deviations from ΔG°_u are much greater than this for RNase T1 and there is no other evidence supporting EX1 behavior. Bai et al. (1994) have proposed that slow proline isomerization could result in hydrogen exchange occurring from a high energy unfolded state. If slow *cis-trans* isomerization dominates under the conditions in which exchange is measured, different values for ΔG°_{op} and ΔG°_u are possible. In equilibrium folding experiments, proline residues will reach their isomeric equilibrium, whereas in HX experiments, a transient population of the globally unfolded state may be sufficient for hydrogen exchange but not proline isomerization. This makes it possible in HX experiments to measure a high energy unfolded state where the proline residues have not had sufficient time to isomerize to the lower energy *trans* conformation. The following equation can be used to describe this free energy difference, $\Delta(\Delta G)$, (Bai et al., 1994):

$$\Delta\Delta G = \Delta G^\circ_{op} - \Delta G^\circ_u = RT\ln(1 + K) \qquad (6)$$

where K is the *cis/trans* proline isomerization constant in the equilibrium unfolded state. RNase T1 has two *cis* prolines in the native conformation, Pro-39 and Pro-55. It has been shown previously in the Schmid laboratory that the complex refolding of RNase T1 is a result of the slow *trans* to *cis* isomerization of these two prolines with the very slowest phase due to the slow isomerization of Pro-39 (Kiefhaber et al., 1990a, 1990b, 1990c, 1992a, 1992b). The microscopic rate constants for proline isomerization as a function of temperature were recently determined for RNase T1 by Mayr et al. (1996). Using their microscopic rate constants, it is possible to estimate a proline isomerization constant, K, for both Pro-39 and Pro-55 as a function of temperature. Modification of Equation 6 to account for the two separate proline isomerizations occurring in RNase T1

$$\Delta\Delta G = \Delta G^\circ_{op} - \Delta G^\circ_u$$
$$= RT\ln(1 + K_{\text{Pro 55}}) + RT\ln(1 + K_{\text{Pro 39}}) \qquad (7)$$

leads to the expected $\Delta\Delta G$ values of 2.6, 2.4, 2.3, and 2.3 kcal/mol at 25, 40, 45, and 50 °C, respectively. Therefore, as shown in Table 3, the measured values of ΔG°_{op} are now in excellent agreement with the measured values of ΔG°_u at all temperatures. From this it appears that in the HX experiments, the "unfolded state" can be described as a higher energy state in which Pro-55 and Pro-39 are still predominantly in the *cis* conformation. In RNase A, a difference of 1.6 to 3 kcal/mol is measured from HX experiments relative to calorimetric or denaturation experiments, respectively (Mayo & Baldwin, 1993; Bai et al., 1994). Bai et al. (1994) computed the expected proline effect on RNase A to be 1.4 kcal/mol, which is similar to the difference observed between HX and calorimetric experiments. The HX data for RNase T1 and RNase A appear to correlate well with exchange occurring from an unfolded state containing *cis* prolines. It is possible, however, that the unfolded states in the various experiments are different, accounting for the differences seen in the free energies calculated from each experiment.

Relationship between hydrogen exchange and exchange pathway

In the two-step model for hydrogen exchange, the observed rate constant for exchange is the sum of the rate constants from the two competing pathways, global unfolding and local fluctuations (Kim & Woodward, 1993; Bai et al., 1994):

$$k_{ex} = k_{ex}(l) + k_{ex}(g) = [K_{op}(l) + K_{op}(g)]k_{int} \qquad (8)$$

$$\Delta G^\circ_{op} = -RT\ln[K_{op}(l) + K_{op}(g)]. \qquad (9)$$

Exchange from the global unfolding pathway is strongly correlated with stability so that when the stability is low most hydrogens will exchange by the global unfolding pathway. Exchange from the local fluctuation pathway is generally less dependent on temperature and pH. It is therefore possible to distinguish between residues that exchange from the two limiting pathways by variation of the temperature.

Table 3. *Comparison of ΔG (D_2O) determined from HX experiments to ΔG (D_2O) from urea denaturation curves*

	pD = 5.6		
	40 °C	45 °C	50 °C
R 77	8.4	7.3	6.2
N 81	8.7	8.0	6.9
Q 85	8.8	7.9	6.7
Average HX ΔG°_{op}	8.6 ± 0.2	7.7 ± 0.4	6.6 ± 0.4
Proline correction[a]	2.4	2.3	2.3
ΔG (D_2O) (HX)[b]	6.2	5.4	4.3
ΔG (D_2O) (urea)[c]	6.9	5.5	4.4

[a] Proline correction = $RT\ln(1 + K_{\text{Pro 55}}) + RT\ln(1 + K_{\text{Pro 39}})$.
[b] ΔG (D_2O) (HX) = Average ΔG° (D_2O) from hydrogen exchange–Proline correction.
[c] ΔG (D_2O) (urea) = ΔG determined in D_2O with urea as the denaturant.

Thirteen residues in RNase T1 have values of ΔG_{op}° that correlate well with exchange occurring from a global unfolding pathway. These residues are all located in the central strands of the β-sheet. As seen in Figure 1, the plot of ln k_{ex} versus $1/T$ for Q85, which is representative of these 13 residues, shows linearity over the measured temperature range giving an activation energy for exchange of 103 kcal/mol. The remaining residues show differing degrees of biphasic behavior indicating varying contributions from the two exchange pathways. In Figure 1, these residues are exemplified by Y11, A19, and T5. When protein stability is high (low temperature), these sites exchange by local unfolding events that have varying temperature dependences, but when protein stability is low (high temperature) all of the residues exchange through the global unfolding pathway. A few residues, S12 and D76, show little temperature dependence for hydrogen exchange, indicating that these residues exchange almost exclusively by limited local fluctuations. If it was possible to go to higher temperature, the exchange kinetics of these residues should converge on the global unfolding path. The remaining residues show intermediate contributions from the two pathways with convergence on the global unfolding pathway at various temperatures. The competition of exchange occurring from one or both of these two pathways reinforces the observation that the central residues of RNase T1 have limited internal motion whereas increasing motion is observed in the adjacent secondary structural units with the greatest degree of motion found in the irregular structure connecting these units.

Relationship between hydrogen exchange and the folding core

In a number of proteins, the very slowest exchanging amides show rapid protection from exchange in rapid-quench hydrogen exchange refolding experiments. This leads to the suggestion that the slowly exchanging hydrogens represent the protein folding core (Kim et al., 1993; Woodward, 1993). Interesting corollaries from this proposal have been presented by Woodward (1993), two of which are: The folding pathway approximates the reverse order of the native state hydrogen exchange rates; and secondary structural segments in the slowly exchanging core determine the overall fold of the protein. Previously, the early folding pathway of RNase T1 was determined by Mullins et al. (1993) utilizing rapid-quench hydrogen exchange, which, along with the data presented here, provides an excellent opportunity to test these proposals. The rapid-quench hydrogen exchange experiments showed a rapid formation of structure throughout RNase T1. There is a direct correspondence between the residues that exhibit the slowest exchange from the native state and those that are rapidly protected during the initiation of folding. All of the slowest exchanging amide residues are located in strands 2–4 of the central β-sheet and these residues are protected first in the early stages of folding. The residues that have somewhat lower rate constants for protection in early folding are predominantly found in the α-helix and the first strand of the small β-sheet. The results of the two experiments are generally consistent, suggesting that the three central strands of the five-stranded β-sheet are important for stability as well as folding. However, the narrow range of rate constants observed for protection from exchange in early folding events makes it difficult to correlate the early folding pathway with the reverse order of native state hydrogen exchange. Finally, it is of interest to note that in both RNase T1 and barnase the slowest exchanging amides are located in the five-stranded β-sheet common to both proteins (Per-

rett et al., 1993). The proteins are in the same nuclease family and have similar functions as well as structure. Is it possible then, that the slowly exchanging five-stranded β-sheet is directing the basic fold of these two proteins?

Materials and methods

Materials

All reagents were purchased from Sigma. RNase T1 was purified as described by Garrett et al. (1995).

Sample preparation and nuclear magnetic resonance spectroscopy

The lyophilized protein was first dissolved in H_2O and allowed to incubate at room temperature for at least 18 h. The samples were then diafiltered and concentrated into either 25 mM acetate-d_3 99.8% D_2O buffer, pD 5.6 or pD 6.6 at 4 °C. Final sample concentrations were 2 mM. The samples were frozen or kept briefly at 4 °C until the commencement of data acquisition. Magnitude COSY spectra were recorded at 25, 40, 45, and 50 °C on a Varian Unity 500 spectrometer and processed with FELIX (Biosym). Typical acquisition parameters were eight transients of 1,024 data points covering 8,000 Hz and 256 t_1 increments with water suppression by presaturation. Prior to Fourier transformation, the data were multiplied by a sine squared function phase shifted by 10° in the t_1 and the t_2 dimension. Crosspeak intensities were measured by volume integration. Each spectrum was internally referenced to two nonexchangeable aromatic crosspeaks (W59 and F80).

Hydrogen exchange

To determine hydrogen exchange rates, magnitude COSY spectra were obtained over various time intervals (14 h at 50 °C to 1 yr at 25 °C) at the specified temperatures. The samples remained in the spectrometer over the time course of all the experiments except for the data collected at 25 °C, where the sample was stored at 25 °C between data acquisitions. Routinely, more than 40 time points were acquired per temperature with the minimal number of time points being 20 at 50 °C. Peak volumes were fit to a single exponential function, $A = A_0[\exp(-kt)] + C$, where C is baseline noise.

Random coil intrinsic exchange rates were calculated as described in Bai et al. (1993) with corrections for temperature and pH utilizing an Excel spreadsheet kindly provided by Andrew Robertson (University of Iowa).

Thermodynamic measurements

Urea denaturation curves were determined in D_2O at 40, 45, and 50 °C for RNase T1 by measuring the intrinsic fluorescence intensity (278 nm excitation and 320 nm emission) of solutions containing approximately 0.9 μM protein as a function of urea concentrations in a thermostated SLM model 8100 fluorometer. The urea was deuterated by repeated lyophilization into D_2O prior to preparation of 8 M urea (50 mM acetate, pD 5.6) stock. The solutions were pre-incubated at the specified temperature for a minimum of 1 h prior to data measurement. The free energy of unfolding was calculated by the linear extrapolation method (Santoro & Bolen, 1988).

Acknowledgments

References

Bai Y, Milne JS, Mayne L, Englander SW. 1993. Primary structure effects on peptide group hydrogen exchange. *Proteins 17*:75–86.

Bai Y, Milne JS, Mayne L, Englander SW. 1994. Protein stability parameters measured by hydrogen exchange. *Proteins Struct Funct Genet 20*:4–14.

Clarke J, Fersht AR. 1996. An evaluation of the use of hydrogen exchange at equilibrium to probe intermediates on the protein folding pathway. *Folding & Design 1*:243–254.

Connelly GP, Bai Y, Jeng MF, Englander SW. 1993. Isotope effects in peptide group hydrogen exchange. *Proteins Struct Funct Genet 17*:87–92.

Englander SW, Kallenbach NR. 1984. Hydrogen exchange and structural dynamics of proteins and nucleic acids. *Q Rev Biophys 16*:521–655.

Englander SW, Mayne L. 1992. Protein folding studied using hydrogen-exchange labeling and two dimensional NMR. *Annu Rev Biophys Biomol Struct 21*:243–265.

Garrett J, Mullins LS, Raushel FM. 1996. Are turns required for the folding of ribonuclease T1? *Protein Sci 5*:204–211.

Hoffman E, Rüterjans H. 1988. Two-dimensional 1H-NMR investigation of ribonuclease T1. *Eur J Biochem 177*:539–560.

Hu CQ, Sturtevant JM, Erickson RE, Pace CN. 1992. Thermodynamics of ribonuclease T1 denaturation. *Biochemistry 31*:4876–4882.

Hvidt A, Nielsen SO. 1966. Hydrogen exchange in proteins. *Adv Protein Chem 21*:287–386.

Jeng MF, Dyson HJ. 1995. Comparison of the hydrogen-exchange behavior of reduced and oxidized *Escherichia coli* thioredoxin. *Biochemistry 34*:611–619.

Johnson JL, Raushel FM. 1996. The influence of primary sequence transpositions on the folding pathways of ribonuclease T1. *Biochemistry 35*:10223–10233.

Kiefhaber T, Grunert HP, Hahn U, Schmid FX. 1990a. Replacement of a *cis* proline simplifies the mechanism of ribonuclease T1 folding. *Biochemistry 29*:6475–6480.

Kiefhaber T, Grunert HP, Hahn U, Schmid FX. 1992a. Folding of RNase T1 is decelerated by a specific tertiary contact in a folding intermediate. *Proteins Struct Funct Genet 12*:171–178.

Kiefhaber T, Quaas R, Hahn U, Schmid FX. 1990b. Folding of ribonuclease T1. 1. Existence of multiple unfolding stated created by proline isomerization. *Biochemistry 29*:3053–3061.

Kiefhaber T, Quaas R, Hahn U, Schmid FX. 1990c. Folding of ribonuclease T1. Kinetic models for the folding and unfolding reactions. *Biochemistry 29*:3061–3070.

Kiefhaber T, Schmid FX, Willaert K, Engelbroughs Y, Chaffottee A. 1992b. Structure of a rapidly formed intermediate in ribonuclease t1 folding. *Protein Sci 1*:1162–1166.

Kim KS, Fuchs, JA, Woodward CK. 1993. Hydrogen exchange identifies native state motional domains important in protein folding. *Biochemistry 32*:9600–9608.

Kim KS, Woodward C. 1993. Protein internal flexibility and global stability: Effect of urea on hydrogen exchange rates of bovine pancreatic trypsin inhibitor. *Biochemistry 32*:9609–9613.

Kraulis PJ. 1991. MOLSCRIPT: A program to produce both detailed and schematic plots of protein structures. *J Applied Crystallography 24*:946–950.

Linderström-Lang KU. 1955. Deuterium exchange between peptides and water. Symposium on Peptide Chemistry. *Chem Soc Spec Publ 2*:1–20.

Loh SN, Prehoda KE, Wang J, Markley JL. 1993. Hydrogen exchange in unligated and ligated staphylococcal nuclease. *Biochemistry 32*:11022–11028.

Loh SN, Rohl CA, Kiefhaber T, Baldwin RL. 1996. A general two-process model describes the hydrogen exchange behavior of RNase A in unfolding conditions. *Proc Natl Acad Sci USA 93*:1982–1987.

Malin R, Zielenkiewicz P, Saenger W. 1991. Structurally conserved water molecules in ribonuclease T1. *J Biol Chem 266*:4848–4852.

Martinez-Oyanedel J, Choe HW, Heinemann U, Saenger W. 1991. Ribonuclease T1 with free recognition and catalytic site: Crystal structure analysis at 1.5 Å resolution. *J Mol Biol 222*:335–352.

Mayo SL, Baldwin RL. 1993. Guanidium chloride induction of partial unfolding in amide proton exchange in RNase A. *Science 262*:873–876.

Mayr LM, Odefey CO, Schutkowski M, Schmid FX. 1996. Kinetic analysis of the unfolding and refolding of ribonuclease T1 by a stopped-flow double-mixing technique. *Biochemistry 35*:5550–5561.

Merritt EA, Murphy MEP. 1994. Raster 3D Version 2.0—A program for photorealistic molecular graphics. *Acta Crystallorg D 50*:869–873.

Molday RS, Englander SW, Kallen RG. 1972. Primary structure effects on peptide group hydrogen exchange. *Biochemistry 11*:150–158.

Mullins LS, Pace CN, Raushel FM. 1993. Investigation of ribonuclease T1 folding intermediates by hydrogen-deuterium amide exchange-two-dimensional NMR spectroscopy. *Biochemistry 32*:6152–6156.

Orban J, Alexander P, Bryan P, Khare D. 1995. Assessment of stability differences in the protein G B1 and B2 domains from hydrogen–deuterium exchange: Comparison with calorimetric data. *Biochemistry 34*:15291–15300.

Pace CN, Heinemann U, Hahn U, Saenger W. 1991. Ribonuclease T1 structure, function, and stability. *Angewandte Chemie 30*:343–454.

Perrett S, Clarke J, Hounslow AM, Fersht AR. 1995. Relationship between equilibrium amide proton exchange behavior and the folding pathway of barnase. *Biochemistry 34*:9288–9298.

Radford SE, Buck M, Topping KD, Dobson CM, Evans PA. 1992. Hydrogen exchange in native and denatured states of hen egg white lysozyme. *Proteins Struct Funct Genet 14*:237–248:

Santoro MM, Bolen DW. 1988. Unfolding free energy changes determined by the linear extrapolation method. 1. Unfolding of phenylmethanesulfonyl α-chymotrypsin using different denaturants. *Biochemistry 27*:8063–8068.

Swint L, Robertson AD. 1993. Thermodynamics of unfolding for turkey ovomucoid third domain: Thermal and chemical denaturation. *Protein Sci 2*:2037–2049.

Swint-Kruse L, Robertson AD. 1996. Temperature and pH dependence of hydrogen exchange and global stability for ovomucoid third domain. *Biochemistry 35*:171–180.

Yu Y, Makhataze GI, Pace CN, Privalov PL. 1994. Energetics of ribonuclease T1 structure. *Biochemistry 33*:3312–3319.

Woodward CK, Simon I, Tuchsen E. 1982. Hydrogen exchange and the dynamic structure of proteins. *Mol Cell Biochem 48*:135–160.

Woodward CK. 1993. Is the slow folding core the protein folding core? *TIBS 18*:359–360.